

Phase and Amplitude Characteristics of InP:Fe Modified Interdigitated Gap Photoconductive Microwave Switches

INGMAR L. ANDERSSON, STUDENT MEMBER, IEEE, AND SVERRE T. ENG, MEMBER, IEEE

Abstract — The transmission amplitude and phase characteristics of InP:Fe modified interdigitated gap (MIG) photoconductive microwave switches are reported. Measurements in the 0.1–1 GHz frequency range show that the phase is shifted $\sim 90^\circ$ and that the corresponding change in amplitude ranges from 43 dB at 0.1 GHz to 23 dB at 1 GHz when the illumination-induced conductance is switched from a low OFF-state value ($\sim 4 \cdot 10^{-8}$ S) to a high ON-state value (5 mS). The observed characteristics can be described by a phase-shifting region and an amplitude modulation region. In the phase-shifting region the phase strongly depends on the conductance, and the amplitude is almost constant. In the amplitude modulation region both the amplitude and the phase depend on the conductance but the effect on the amplitude is much more pronounced. A lumped-element model describing the device performance is presented. It is concluded that these optoelectronic microwave switching devices are suitable for high-speed amplitude modulation but are not too promising as high-speed phase shifters.

I. INTRODUCTION

THE USE OF laser-controlled solid-state devices in high-speed signal processing is a subject of continuing interest. One of the devices that has received the most attention is the picosecond photoconductive switch, first demonstrated in Si [1] and later in GaAs [2] and InP [3]. These types of switches have been proposed and successfully used for the high-speed switching of electrical signals ranging from dc [1]–[3] up to the GHz range [4]–[7]. Other applications include high-voltage short pulse generation [8]–[9], high-speed sampling [10]–[12], and the generation of high-frequency waveforms [13]–[15]. In comparison with conventional electronic switching devices, these optoelectronic devices are relatively simple to fabricate and offer significant improvements in both switching speed and power handling. Optical fibers can be used for distributing the control signal, and an inherently high isolation will be obtained. Thus, the introduction of these devices into microwave systems may lead to new applications and designs where high speed, low weight, and low cost are of the utmost importance (e.g. future airborne radars).

Manuscript received May 17, 1988; revised October 31, 1988. This work was supported by the National Swedish Board for Technical Development.

The authors are with the Department of Optoelectronics and Electrical Measurements, Chalmers University of Technology, S-412 96 Gothenburg, Sweden. S. T. Eng has a joint appointment with the Jet Propulsion Laboratory, California Institute of Technology, Pasadena, CA 91109.

IEEE Log Number 8826045.

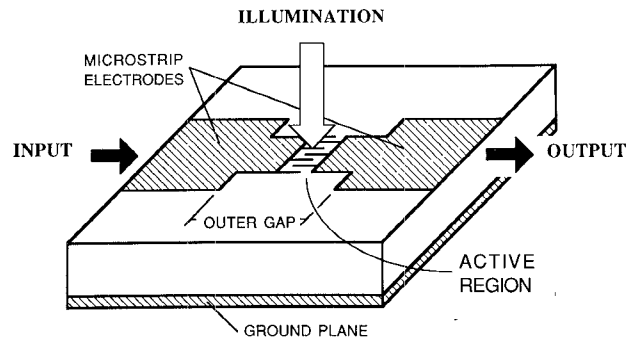


Fig. 1. Schematic illustration of a modified interdigitated gap (MIG) photoconductive microwave switch.

The most widely used device structures have active regions formed by a single gap discontinuity (SG) in a microstrip transmission line deposited onto a high-resistivity semiconductor material. Modulation or switching is achieved by focusing the controlling laser beam onto the active region. Because of the intrinsic capacitances associated with the gap discontinuity, the illumination will switch the transmission from a capacitive OFF state to a conductive ON state. As a result, the transmitted signal will change in both amplitude and phase during the switching operation. Since both amplitude and phase control are important building blocks in today's microwave systems and those proposed for the future, knowledge of the amplitude and the phase of the transmitted signal is of vital importance.

In this paper we report an investigation of the transmission amplitude and phase characteristics in the 0.1–1 GHz frequency range for an InP:Fe based modified interdigitated gap (MIG) photoconductive microwave switch. This device structure, which is schematically illustrated in Fig. 1, has been presented elsewhere and has been shown to reduce the effective gap capacitances and thereby improve the amplitude modulation performance [6]. Because of the interdigitated active region the device is also more efficient than the commonly used SG devices when using optical fibers for illumination. The measurements show that both the amplitude and the phase of the transmitted signal strongly depend on the illumination-induced conductance.

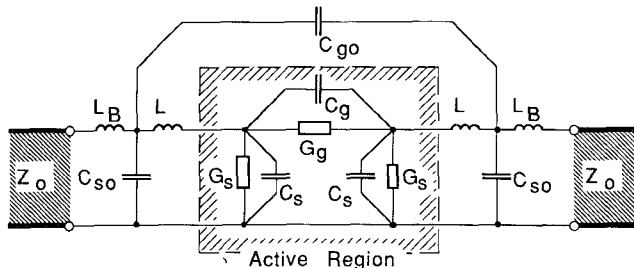


Fig. 2. Equivalent lumped circuit model for a MIG device.

The observed characteristics can be described by two regions. Up to a certain frequency-dependent threshold value, the phase depends strongly on the conductance while the transmitted amplitude is almost constant and low. As a result, this region can be called the phase-shifting region. For conductances above this threshold value both the amplitude and the phase depend on the conductance but the effect on the amplitude is much more pronounced. Consequently, this region can be called the amplitude modulation region. A lumped-element model for describing the device performance is also presented. From the results, it is concluded that these optoelectronic microwave devices are suitable for high-speed amplitude modulation but are not promising as high-speed phase shifters. To our knowledge this is the first reported investigation of the phase and amplitude characteristics of these types of devices.

II. MODEL

A rigorous analysis of the MIG device performance is difficult to make. However, because of the small device dimensions compared with the operating frequency microstrip wavelength, the microwave performance can be modeled by the equivalent lumped circuit [4], [16]. The model used for the MIG device is shown in Fig. 2. C_g , C_s , C_{go} , and C_{so} represent the gap and shunt capacitances associated with the active region and the outer gap, respectively. G_g and G_s are the gap and shunt conductances, which depend on both the illumination intensity and the wavelength. By using high-resistivity materials and proper illumination wavelengths, yielding a very thin photoexcited surface layer, G_s can be neglected [16]. L and L_B correspond to the inductances of the narrow microstrip lines and the bonding wires (if used), respectively.

Based on the S -parameter concept, the microwave transmission can be calculated from the transmission coefficient S_{21} . The general analytic expression for a MIG device, which is presented in the Appendix, is fairly complicated. However, if the influence of L is small, it is possible to describe the MIG device by a modified SG device model through the introduction of effective gap and shunt capacitances (see the Appendix). In this case, the transmission coefficient for a MIG device can be expressed as ($G_s = 0$)

$$S_{21} = \frac{2Z_0(G_g + j\omega C_{g,\text{eff}})}{[1 + (Z_0 + j\omega L_B)j\omega C_{s,\text{eff}}][1 + (Z_0 + j\omega L_B)(2G_g + j\omega(2C_{g,\text{eff}} + C_{s,\text{eff}}))]} \quad (1)$$

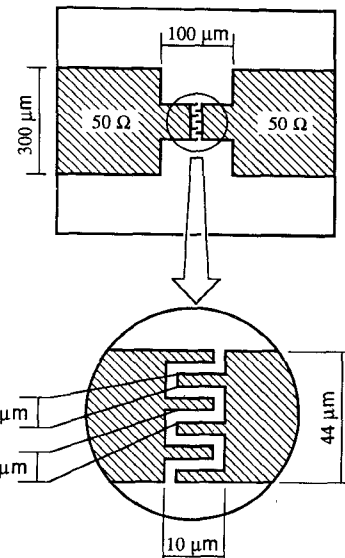


Fig. 3. Top view presentation of the experimentally tested MIG device structure.

where ω is the angular frequency of the microwave signal, Z_0 is the characteristic impedance, $C_{g,\text{eff}} = C_g + C_{go}$, and $C_{s,\text{eff}} = C_s + C_{so}$.

The shunt capacitances, which will degrade the performance, can be minimized by careful design of the device [17]. The gap conductance under constant illumination can be calculated from (assuming uniform electron-dominated current flow and no contact resistance)

$$G_g = \eta(1 - R)\mu\tau_e \frac{e}{h\nu} \frac{IA_e}{s^2} \quad (2)$$

where η is the quantum efficiency, R is the surface reflectivity, μ is the electron mobility, τ_e is the effective excess carrier lifetime, e is the electronic charge, $h\nu$ is the photon energy, s is the interdigital electrode spacing (gap), A_e is the effectively illuminated area of the active region, and I is the optical intensity.

From (1) it is possible to calculate both the amplitude and the phase of the transmitted signal. In the OFF state, where the gap conductance is low (generally $< 10^{-7}$ S), the transmission is controlled by the effective gap capacitances, and the phase is almost 90° , with reference to the incident signal. As the illumination intensity is increased, the gap conductance increases and the transmission will gradually switch to a conductance-controlled state ($G_g > \omega C_{g,\text{eff}}$) where the phase approaches 0° . Thus, the phase of the transmitted signal will change by approximately 90° when switching the illumination from a low to a high conductance state.

III. EXPERIMENTS

Fig. 3 is a top view illustration of the MIG device structure used in this work. Following conventional cleaning and etching procedures, the MIG electrode structures

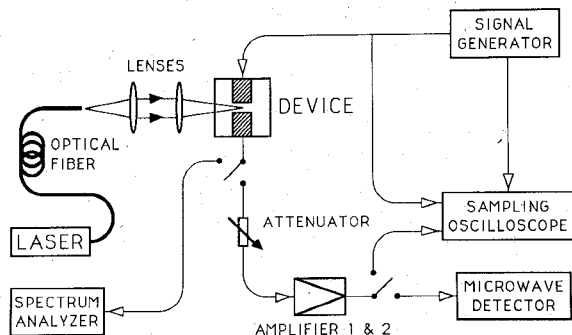


Fig. 4. Block diagram of the experimental setup.

of Au:Ge/Ni/Au were patterned onto $\sim 400\text{-}\mu\text{m}$ -thick slices of semi-insulating Fe-doped InP ($\rho > 10^7 \Omega\cdot\text{cm}$) using vacuum evaporation and lift-off techniques. The width of the microstrip electrodes was designed to maintain the 50Ω geometry ($\sim 300\text{ }\mu\text{m}$). The electrode spacing (gap) was $4\text{ }\mu\text{m}$, and the interdigital electrode lines were $4\text{ }\mu\text{m}$ wide and $6\text{ }\mu\text{m}$ long. The overall active region measured $10\text{ }\mu\text{m} \times 44\text{ }\mu\text{m}$ and the outer gap was $100\text{ }\mu\text{m}$ long. The slices were alloyed for ohmic contacts and cleaved into individual devices ($1\text{ mm} \times 1\text{ mm}$). The individual devices were cemented to aluminum blocks and wire bonded to microstrip lines for evaluation.

Fig. 4 shows a block diagram of the experimental setup. A high-power GaAlAs/GaAs semiconductor laser (Spectra Diode Labs SDL-2410-H2) emitting at 805 nm , with a fiber pigtail ($100\text{ }\mu\text{m}$ core) and a maximum CW output of 50 mW , was used for illumination. The fiber output was imaged on the active region in a $1:1$ scale by lenses, which corresponds to a fiber-to-device butt-coupling situation. Both the amplitude and the phase of the transmitted signal were measured at different illumination-induced conductance values and for different frequencies. The amplitude was measured with a microwave power detector (Philips PM 7520). A double amplifier stage was used because of initially low transmission levels. At high transmission levels, the variable attenuator prior to the amplifier stage was used in order to prevent the amplifiers from reaching saturation. For comparison purposes, the signal power could also be measured using a spectrum analyzer. The phase was obtained by measuring the relative phase difference of the transmitted signal and a reference signal. The conductance values corresponding to each illumination intensity were calculated from measurements of the voltage appearing at an output load resistance when a dc voltage was applied to the input of the device. These values have also been confirmed by I/V measurements.

IV. RESULTS AND DISCUSSIONS

Figs. 5 and 6 show measured amplitude ($|S_{21}|$) and phase ($\angle S_{21}$) of the transmitted signal with respect to the input signal as a function of conductance for four frequencies ($0.1, 0.25, 0.5, \text{ and } 1\text{ GHz}$). Since L is about 50 pH , the maximum gap conductance is 5 mS , and the gap capacitances are of the order of 50 fF or less [17] for our device, the use of (1) for modeling the MIG device is justified (see

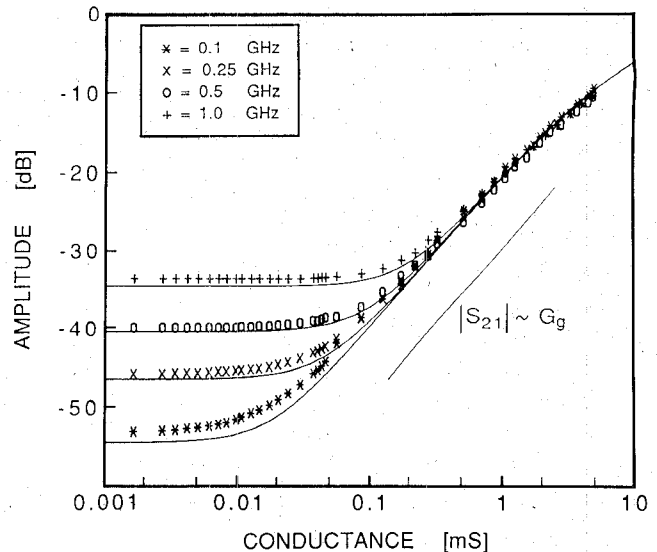


Fig. 5. Measured and calculated (solid lines) amplitude transmission versus conductance.

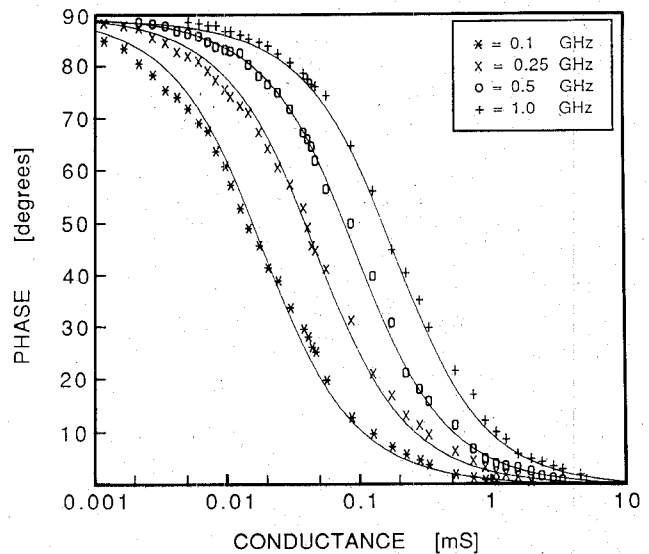


Fig. 6. Measured and calculated (solid lines) phase of the transmitted signal versus conductance.

(A4) and (A5) in the Appendix). Based on the assumptions that $\omega L_B \ll Z_0$ and $G_g, \omega C_{g,\text{eff}} \ll (2Z_0)^{-1}$, one can see that the amplitude transmission will increase by 3 dB when $G_g = \omega C_{g,\text{eff}}$ (amplitude modulation threshold). Fig. 5 shows that the latter assumptions are justified, and since L_B is calculated to be less than 150 pH it is possible to estimate the effective gap capacitance from the frequency-dependent threshold values. The theoretical curves (solid lines) have been calculated from (1) using $Z_0 = 50\Omega$, $C_{g,\text{eff}} = 30\text{ fF}$, and $C_{s,\text{eff}}, L_B = 0$. The value for the effective gap capacitance has been estimated from the measured amplitude modulation threshold values. This value has also been confirmed by OFF state transmission measurements in the $0.01\text{--}1\text{ GHz}$ frequency range. The good agreement between measured and calculated values implies that the model describes the performance well. It is, however, necessary to point out that the modified SG model representa-

tion of the MIG device can only be applied if L is negligibly small.

As mentioned above, Fig. 5 shows that the conductance has to overcome a threshold value, set by the effective gap capacitance and the operating frequency, before the transmitted amplitude starts to increase. As the conductance is increased further, the amplitude will continue to increase and if the threshold value is sufficiently low, it will pass through a linear region ($|S_{21}| \sim G_g$) and then gradually approach the maximum transmission level (0 dB). A maximum ON-state conductance of 5 mS and a corresponding transmission of -10 dB were measured. These values were obtained with an illumination intensity of 700 W/cm^2 (50 mW from the fiber), and the measured conductance value is about a factor of 2 lower than one would calculate from the first-order model (2) for this optical intensity (using $\eta = 100$ percent, $h\nu = 1.54 \text{ eV}$, $R = 28$ percent, $\mu = 2000 \text{ cm}^2/\text{Vs}$, $\tau_e = 1 \text{ ns}$, and $A_e = 3 \cdot 10^{-6} \text{ cm}^2$). The dynamic switching range (illumination on/off modulation) can also be seen. It varies from 43 dB at 0.1 GHz to 23 dB at 1 GHz. The illumination efficiency ($A_e/A_{\text{fiber core}}$) is ~ 4 percent, which corresponds to an effective optical power of $\sim 2 \text{ mW}$. More efficient illumination, i.e., higher effective optical power, will improve the ON-state transmission and thereby the dynamic switching range. The transmission at low conductance values, which corresponds to the OFF-state signal leakage, indicates that the ultimate dynamic switching range is about 10 dB higher than the values measured here. However, since the transmitted amplitude characteristics begin to deviate from the linear behavior at about -20 dB (see Fig. 5), the increase in the ON-state transmission from -10 dB to -4 dB, i.e., by a factor of 2, will require an effective optical power about four times higher ($\sim 8 \text{ mW}$). Although these numbers may not seem too promising, it would be possible to obtain an ON-state transmission of about 93 percent (-0.6 dB) for the present device if the total output power from the fiber were focused on the active region. Further improvements of the dynamic switching range can be obtained by reducing the effective gap capacitances, which will decrease the residual OFF state transmission and shift the amplitude modulation

and the incident signals are in phase. This is expected since at high conductance values the gap is virtually short-circuited.

Using the transmission coefficient given by (1), it is possible to show that for operating frequencies causing OFF-state transmissions of less than -20 dB, the initial phase is more than 80° . This situation corresponds to about 5 GHz for our operating conditions. Consequently, a device where the amplitude is switched more than 20 dB (on/off) will have a corresponding phase shift of 80° or more.

V. CONCLUSIONS

The transmission characteristics for InP:Fe based modified interdigitated gap (MIG) photoconductive microwave switches have been investigated in the 0.1–1 GHz frequency range. Both the amplitude and the phase have been measured as a function of illumination-induced conductance. The good agreement between measured and calculated values indicates that the proposed model describes the performance of the MIG device well. The experimental data show that the phase will shift almost 90° when the amplitude is switched more than 20 dB (on/off). For conductance values up to the threshold value, the phase will change to a value corresponding to approximately half its initial value, and the amplitude is virtually constant. This region may be referred to as the phase-shifting region. However, the amplitude is low and it is doubtful if the phase shifting properties can be used. When the conductance is increased further, the amplitude increases rapidly until it begins to saturate. Consequently, this region may be called the amplitude modulation region. The results show that devices of this type are suitable for high-speed amplitude switching or modulation but are not too promising as high-speed phase shifters. Although the measurements have been carried out for a InP:Fe based device, the results are applicable to similar devices based on other high-resistivity materials.

APPENDIX

The general complex transmission S_{21} coefficient for a MIG device, described by the model in Fig. 2, is given by

$$S_{21} = \frac{1}{P + (Z_0 + j\omega L_B)(G_s + j\omega(C_s + C_{so}P))} \cdot \frac{2Z_0P[G_g + j\omega(C_g + C_{go}PQ)]}{PQ + (Z_0 + j\omega L_B)[2G_g + G_sQ + j\omega[2(C_g + C_{go}PQ) + (C_s + C_{so}P)Q]]} \quad (A1)$$

threshold to lower conductance values. However, no effect on the ON-state transmission will be obtained by doing so.

Fig. 6 shows that the initial phase of the transmitted signal is close to 90° . As the conductance is increased, the phase starts to change, beginning at conductance values about an order of magnitude lower than the threshold values for amplitude modulation. At the amplitude modulation threshold it has a value corresponding to approximately half its initial value and it gradually approaches 0° for high conductance values. In this case the transmitted

where

$$P = 1 - \omega^2 LC_s + j\omega LG_s \quad (A2)$$

and

$$Q = 1 - \omega^2 L(2C_g + C_s) + j\omega L(2G_g + G_s). \quad (A3)$$

It is possible to show that both the P and the Q parameters will degrade the high-frequency performance and that minimum degradation will be obtained if P and Q are

close to unity. Since $G_g \gg G_s$ for efficient switching [16] and $C_g \gg C_s$ for small size active region design [17], the Q parameter will have a stronger influence on the characteristics. Consequently, the degradation effect will be negligibly small if

$$\omega L \ll [\omega (2C_g + C_s)]^{-1} \quad (A4)$$

and

$$\omega L \ll [2G_g + G_s]^{-1}. \quad (A5)$$

If these conditions are satisfied, (A1) reduces to the simplified expression

$$S_{21} = \frac{1}{1 + (Z_0 + j\omega L_B)[G_s + j\omega(C_s + C_{so})]} \times \frac{2Z_0(G_g + j\omega(C_g + C_{go}))}{1 + (Z_0 + j\omega L_B)[2G_g + G_s + j\omega[2(C_g + C_{go}) + C_s + C_{so}]]}. \quad (A6)$$

By putting $L_B = C_{go} = C_{so} = 0$, (A6) reduces to the S_{21} coefficient for a single gap discontinuity (SG) device as given by Platte [16]. Thus if the inductance of the narrow microstrip lines is sufficiently small (see (A4) and (A5)), it is possible to describe the MIG device by a modified SG device model.

ACKNOWLEDGMENT

The authors wish to thank Dr. A. Larsson and Dr. P. Andersson for stimulating discussions and for reading the manuscript.

REFERENCES

- [1] D. H. Auston, "Picosecond optoelectronic switching and gating in silicon," *Appl. Phys. Lett.*, vol. 26, pp. 101-103, Feb. 1975.
- [2] R. A. Lawton and A. Scavanne, "Photoconductive detector of fast-transition optical waveforms," *Electron. Lett.*, vol. 11, pp. 74-75, Feb. 1975.
- [3] F. J. Leonberger and P. F. Moulton, "High-speed InP optoelectronic switch," *Appl. Phys. Lett.*, vol. 40, pp. 447-449, Nov. 1979.
- [4] A. M. Johnson and D. H. Auston, "Microwave switching by picosecond photoconductivity," *IEEE J. Quantum Electron.*, vol. QE-11, pp. 283-287, June 1975.
- [5] F. Platte and G. Appelhaus, "Optoelectronic gating of microwave signals using a silicon microstrip shunt modulator," *Electron. Lett.*, vol. 12, pp. 270-271, May 1976.
- [6] I. Andersson and S. T. Eng, "High-speed control of microwave signals using InP:Fe photoconductive devices," in *Proc. 17th European Solid State Device Res. Conf.* (Bologna, Italy), Sept. 1987, pp. 1073-1076.
- [7] I. Andersson and S. T. Eng, "Analysis of a high-speed laser-controlled microstrip directional coupler," *Solid-State Electron.*, vol. 30, pp. 133-137, Jan. 1987.
- [8] C. H. Lee, "Picosecond optoelectronic switching in GaAs," *Appl. Phys. Lett.*, vol. 30, pp. 84-86, Jan. 1977.
- [9] P. LeFur and D. H. Auston, "A kilovolt picosecond optoelectronic switch and a Pockels cell," *Appl. Phys. Lett.*, vol. 28, pp. 21-23, Jan. 1976.
- [10] A. Antonetti, A. Migu, M. M. Malley, and G. Mourou, "Optoelectronic sampling in the picosecond range," *Opt. Commun.*, vol. 21, pp. 211-214, May 1977.
- [11] A. J. Low and J. E. Carroll, "10 ps optoelectronic sampling system," *Solid-State and Electron Devices*, vol. 2, pp. 185-190, Nov. 1978.
- [12] D. H. Auston, A. M. Johnson, P. R. Smith, and J. C. Bean, "Picosecond optoelectronic detection, sampling, and correlation

measurements in amorphous semiconductors," *Appl. Phys. Lett.*, vol. 37, pp. 371-373, Aug. 1980.

- [13] J. M. Proud and S. L. Norman, "High-frequency waveform generation using optoelectronic switching in silicon," *IEEE Trans. Microwave Theory Tech.*, vol. MTT-26, pp. 137-140, Mar. 1978.
- [14] G. Mourou, C. V. Stancampiano, and D. Blumenthal, "Picosecond microwave pulse generation," *Appl. Phys. Lett.*, vol. 38, pp. 470-472, Mar. 1981.
- [15] P. Paulus, W. Brinker, and D. Jäger, "Generation of microwave pulses by optoelectronically switched resonators," *IEEE J. Quantum Electron.*, vol. QE-22, pp. 108-111, Jan. 1986.
- [16] W. Platte, "Spectral dependence of microwave power transmission in laser-controlled solid-state microstrip switches," *Solid-State and Electronic Devices*, vol. 2, pp. 97-103, July 1978.
- [17] Y. Rahmat-Samii, T. Itoh, and R. Mittra, "A spectral domain analysis for solving discontinuity problems," *IEEE Trans. Microwave Theory Tech.*, vol. MTT-22, pp. 372-378, Apr. 1974.

✉

Ingmar L. Andersson (S'83) was born in Karlstad, Sweden, on November 19, 1957. He received the M.S. degree in engineering physics from Chalmers University of Technology, Gothenburg, Sweden, in 1982.

In 1982 he joined the Research Laboratory at the Department of Optoelectronics and Electrical Measurements, Chalmers University of Technology, where he is currently pursuing the Ph.D. degree. His current research interests are in high-speed optoelectronic devices and their application to integrated microwave circuits and systems.

✉

Sverre T. Eng (M'58) received the M.S. degree in electrical engineering in 1953 and the Ph.D. degree in applied physics in 1967, both from Chalmers University of Technology, Gothenburg, Sweden.

From 1953 to 1956 he was engaged in the research and development of ultrasensitive microwave receivers for radio astronomy at Chalmers University of Technology. He later (1956-1967) spent ten years at Hughes Research Laboratories, Newport Beach, CA, as a Member of the Technical Staff, Section Head and Department Head, where he built up a research department in microwave and optical solid-state electronics. He initiated research on parametric diodes, mixers, tunnel diodes, optical detectors, semiconductor lasers, and instrumentation. In 1967 he joined North American Rockwell Corporation, Anaheim, CA, and spent four years conducting research on lasers and electro-optic systems. Since 1971, he has been Professor and Director of the Department of Optoelectronics and Electrical Measurements, Chalmers University of Technology, where he has conducted research on fiber-optics communication, applied laser spectroscopy, and optical and digital computers in scientific instrumentation. On leave from Chalmers University of Technology, he has worked as a consultant and Division Technologist at the Jet Propulsion Laboratory, California Institute of Technology, Pasadena, CA, in the areas of long-range R&D planning, fiber optics, integrated optics, and optical information processing research. He is the author of more than 100 technical publications and has several patents.

Dr. Eng is a member of the Royal Swedish Academy of Engineering Sciences, APS, and OSA.



Ingmar L. Andersson

✉

✉